

# Influence Of Extended Defect Models On Prediction Of Boron Transient Enhanced Diffusion

Srinivasan Chakravarthi<sup>†</sup> and Scott T. Dunham<sup>‡</sup>

<sup>†</sup> Department of Manufacturing Engineering

<sup>‡</sup> Department of Electrical and Computer Engineering  
Boston University, Boston, MA 02215, srini@bu.edu

Implantation induced Transient Enhanced Diffusion is a complex process involving multiple interactions between dopants, point and extended defects. Effective modeling of TED requires an understanding of all these interactions. Frequently to simplify the system, modelers use assumptions such as the '+1' model for their initial conditions. For extended defects, a range of models based on solid solubility, discrete clusters or the moments of the size distribution have been used. In this paper we evaluate some of these modeling choices by comparing model prediction to boron TED data.

## INTRODUCTION

Ion implantation is a widely used technique for introducing dopant atoms in Si. It is well known that implantation introduces damage that on annealing leads to the phenomenon of transient enhanced diffusion (TED). Implantation introduces a large number of point defects orders of magnitude higher than the dopant concentration. These excess interstitials and vacancies recombine with each other during the initial stages of annealing. The remaining point defects interact with the dopant via coupled diffusion. Excess point-defects also form extended defects, primarily {311} defects for interstitials and boron interstitial clusters (BICs) for boron.<sup>1,2</sup> There have been different approaches in the past to modeling this system.<sup>3,4,5</sup> In this paper we evaluate the effectiveness of various assumptions and models in predicting TED of boron.

## INITIAL DAMAGE

Each implanted ion creates a defect cascade, producing a large number of interstitials and vacancies. Fig. 1 shows a typical set of defect and dopant profiles from TRIM,<sup>6</sup> a Monte Carlo ion implantation simulator. Although the large initial interstitial and vacancy profiles are nearly equal, subtracting them reveals that the surface is vacancy rich while interstitials are kicked deeper into the substrate, with the integrated net I-V dose approximately equal to the implant dose. For lighter ions like boron where the displacement between interstitials and vacancies is small, a '+1' model has appeared to be a reasonable approximation,<sup>7</sup> and there has been considerable success in modeling TED using this simple model. However, we have found that there is considerable under-estimation of diffusion using this approach for low implant doses.<sup>8</sup> This is because when the defect density is relatively small, the faster diffusing species can reach the surface before encountering the opposite type defect. Since based on *ab initio* calculations,<sup>9</sup> vacancies diffuse faster than interstitials, they are annihilated at the surface more often leading to a net 'plus' value greater than one as shown in Fig. 2. The simulations were done using a continuum diffusion simulator that used the full interstitial and vacancy distribution from TRIM as inputs. It may be noted that for moderate or high implant doses I/V recombination quickly leads to a approximately '+1' distribution, validating the effectiveness of the '+1' approach.

## COUPLED DIFFUSION

It is well known that dopants migrate and interact with point-defects by coupled diffusion.<sup>10</sup> We use a five-stream approach for our simulation of dopant diffusion<sup>10</sup> as implemented in the process simulator PMM/DOPDEES.<sup>11</sup> The boron diffusivity parameters are based on iso-concentration

experiments<sup>12</sup> and the point defect parameters are based on metal diffusion experiments and atomistic calculations.<sup>9</sup> The {311} models used for comparison are a simple kinetic solubility model<sup>13</sup> and a moment-based model.<sup>8</sup>

## DOPANT/INTERSTITIAL INTERACTIONS

Because of its size, boron aggregates together with silicon interstitials to form immobile boron interstitial cluster (BICs). As illustrated in Fig. 3, there is a huge array of potential cluster compositions. It is possible to model this system with a variety of approaches. Examples include either cluster-based and a moment-based approaches. Cluster models consider a subset of discrete smaller sized clusters, whereas moment-based models like KPM<sup>14</sup> consider larger cluster sizes but make assumption about smooth changes in properties with size and limits the system to a narrower range of compositions.

### Cluster Model

The cluster model implemented in this work uses kinetic reactions that lead to the formation of clusters. For example, a substitutional boron can react with a silicon self interstitial to form an immobile BI which can further react with another interstitial to form a BI<sub>2</sub> cluster or with an interstitial boron (B<sub>i</sub>) to give B<sub>2</sub>I<sub>2</sub>. For reactions of the form  $A + B \rightleftharpoons C$ , the rate of formation of C is given by,

$$R = 4\pi r_{\text{cap}}(D_A + D_B)(C_A C_B - \frac{C_C}{K_{\text{eq}}}) \quad (1)$$

where  $r_{\text{cap}}$  is the capture radius of the reaction and  $D$  and  $C$  represent diffusivity and concentration. Cluster energetics calculations from Zhu *et al.*<sup>15</sup> were used as the basis for the simulations. The model uses 10 different clusters: BI, BI<sub>2</sub>, B<sub>2</sub>I, B<sub>2</sub>I<sub>2</sub>, B<sub>3</sub>I, B<sub>3</sub>I<sub>2</sub>, B<sub>4</sub>I<sub>2</sub>, B<sub>4</sub>I, B<sub>2</sub>, B<sub>3</sub>. BI<sub>2</sub> seems to be the main cluster species for short times (1 $\mu$ s). For longer times the dominant species is B<sub>3</sub>I.

### Kinetic Precipitation Model

The aggregation process is driven by the minimization of the change in free energy with clustering. This energy can be written as the sum of a volume term which represents the change in energy upon adding either a boron or interstitial to the B<sub>n</sub>I<sub>m</sub> cluster, plus the excess surface energy and strain energies associated with finite size precipitates:

$$\Delta G_{n,m} = -nkT \ln \left( \frac{C_B}{C_B^{ss}} \right) - mkT \ln \left( \frac{C_I}{C_I^{ss}} \right) + \Delta G_{n,m}^{\text{surf}} + \Delta G_{n,m}^{\text{stress}}, \quad (2)$$

We assume that the excess surface energy is a smooth function of size given by

$$\Delta G_{n,m}^{\text{surf}} = c_1 n^{a_1} + c_2 n^{a_2} \quad (3)$$

where  $1 > a_1 > a_2 > \dots$ . The first term corresponds to the asymptotic behavior at large sizes, which is generally associated with the dependence of the active surface area on size (BICs are assumed to be spherical and hence  $a_1 = 2/3$ ), and the other terms are corrections for the deviation of the free energy from this asymptotic behavior at small sizes. The stress energy can be found from elasticity theory to be of the form,

$$\Delta G_{n,m}^{\text{stress}} = H_n + \frac{\alpha}{n}(m - \gamma n)^2. \quad (4)$$

If there were no point defect supersaturation, the optimum number of incorporated interstitials would be  $m^* = \gamma n$ . However, when  $C_I > C_I^*$ , the optimum number of point defects incorporated can be found by minimizing the free energy to be:

$$m^* = n \left( \gamma + \frac{kT}{2\alpha} \log(C_I/C_I^*) \right), \quad (5)$$

which leads to an effective solid solubility of:

$$C_{\text{ss}}^{\text{eff}} = C_{\text{ss}} \left( \frac{C_1}{C_1^*} \right)^{-\gamma} \exp \left[ -\frac{kT}{4\alpha} (\log(C_1/C_1^*))^2 \right]. \quad (6)$$

It is evident from the above equation that the effective solubility decreases with increase in interstitial super-saturation as observed experimentally.

## SIMULATION RESULTS

### Low Dose TED

Experiments have shown that TED scales non-linearly with dose and seems to almost saturate at low doses. This behavior cannot be satisfactorily explained using a '+1' model. We found that using the '+n' factor obtained from simulations of the full I and V profiles along with fast vacancy diffusion satisfactorily explains the dose dependence of boron marker layer experiments for silicon implants<sup>16</sup> as shown in Fig. 4. As shown in Fig. 5, using this same methodology for boron TED, we can successfully predict low dose TED, while using a '+1' model under-estimates the total amount of diffusion. For low dose simulations, clustering is minimal and the model used for BICs has little or no impact.

### Medium Dose Boron TED

At medium to high doses, boron clustering is the predominant effect. Hence, we can simulate this system using either KPM or cluster models. We optimised both models over TED SIMS data from Intel.<sup>17</sup> It was found that both the cluster and the moment-based models can reasonably model boron TED data over a range of experimental condition, although KPM does seem to show slightly better fits to the data compared to the cluster model. We found satisfactory fits for implant energies from 20 – 80 keV and doses of  $10^{13} - 2 \times 10^{14} \text{ cm}^{-2}$ . Similarly we found good results over a wide temperature range (700 – 1000 °C). Some of these fits are shown in Figs. 6–8.

### {311} Models

The excess interstitials that remain after the initial recombination quickly cluster to form {311} defects. These {311} defects govern the time evolution of the local interstitial concentration  $C_1$  which is directly reflected in the time evolution of the enhanced tail diffusion and effective solubility of boron. Fig. 9 shows a comparison between using a simple solubility model for {311} defects versus a moment-based model which considers ripening.<sup>8</sup> It is clear that the models predict different time evolution of the boron profiles. The simple solid solubility model predicts uniform diffusion as  $C_1$  remains a constant during dissolution of {311}s, whereas the moment-based model shows a faster initial diffusion, followed by slower but longer lasting TED. As is evident in Fig. 9, the fixed solubility model does not capture the observed TED kinetics. In addition, there is a change in effective solid solubility of boron over time. The moment-based model captures the increase in effective boron solubility as  $C_1$  decreases (Eq. 6), while the simple solubility model predicts too low a solubility for longer times because  $C_1$  remains high.

## CONCLUSIONS

We evaluated the effect of the various assumptions and models used for predicting boron TED. It was found that for low doses, the initial interstitial/vacancy recombination plays an important role, leading to a '+n' behavior. This also supports the results of atomistic calculation which conclude that vacancies diffuse faster than interstitials. For medium/high boron doses, a boron clustering model is essential. We found that consideration of either a finite set of discrete clusters or a moment-based model such as KPM can match experimental data satisfactorily for medium doses. A model for {311} which considers the drop in  $C_1$  during annealing (e.g. a moment-based

approach) was found necessary for predicting the time dependence of tail diffusion and effective solubility for the boron profiles.

This work was supported by the Semiconductor Research Corporation.

- 
- <sup>1</sup>D.J. Eaglesham, P.A. Stolk, H.J. Gossmann, and J.M. Poate, *Appl. Phys. Lett.* **65**, 2305 (1994).  
<sup>2</sup>D.J. Eaglesham, P.A. Stolk, H.J. Gossmann, T.E. Haynes, and J.M. Poate, *Nuc. Inst. and Meth. B* **106**, 191 (1995).  
<sup>3</sup>L. Pelaz, M. Jaraiz, G. H. Gilmer, H. J. Gossmann, C. S. Rafferty, and D. J. Eaglesham, *Appl. Phys. Lett.* **70**, 2285 (1991).  
<sup>4</sup>A.D. Lilak, S.K. Earles, K.S. Jones, M. E. Law, and M. D. Giles, in **IEDM Technical Digest**, 493 (1997).  
<sup>5</sup>A.H. Gencer, S. Chakravarthi, and S.T. Dunham, in **SISPAD '97 Proceedings**, (1997).  
<sup>6</sup>O. Vancauwenberghe, N. Herbots, and O. Hellman, *J. Vac. Sci. Tech. B* **9**, 2027 (1991).  
<sup>7</sup>M.D. Giles, *J. Electrochem. Soc.* **138**, 1160 (1991).  
<sup>8</sup>A.H. Gencer and S.T. Dunham, *J. Appl. Phys.* **81**, 631 (1997).  
<sup>9</sup>M. Tang, J. Zhu, and T. Diaz de la Rubia, *Phys. Rev. B* **55**, 14279 (1997).  
<sup>10</sup>S. T. Dunham, *J. Electrochem. Soc.* **139**, 2628 (1992).  
<sup>11</sup>A.H. Gencer. *PMM User's Manual*, <http://eng.bu.edu/~alp/pmm/>, (1997).  
<sup>12</sup>F. Wittel, PhD thesis, Boston University (1995).  
<sup>13</sup>C.S. Rafferty, G.H. Gilmer, M. Jaraiz, D. Eaglesham, and H.J. Gossmann, *Appl. Phys. Lett.* **68**, 2395 (1996).  
<sup>14</sup>I. Clejan and S.T. Dunham, *J. Appl. Phys.* **78**, 7327 (1995).  
<sup>15</sup>J. Zhu, M.-J. Caturla, M. Johnson, and T.D. de la Rubia. Private communication.  
<sup>16</sup>P.A. Packan and J.D. Plummer, *Appl. Phys. Lett.* **56**, 1787 (1990).  
<sup>17</sup>TED SIMS data from Intel Corporation.

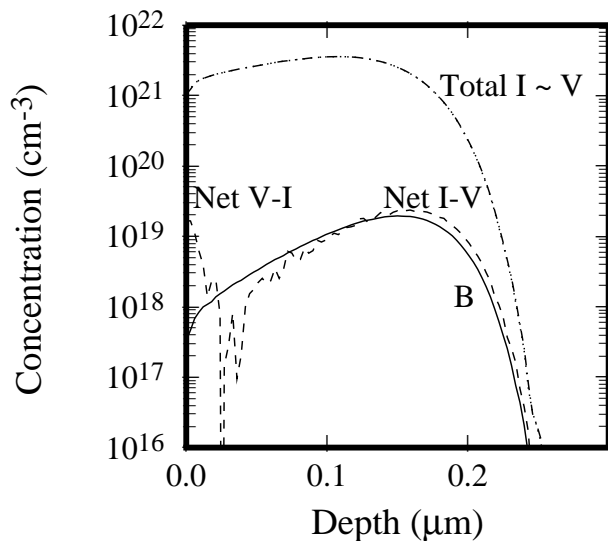


**Fig. 1:** Monte Carlo simulation showing initial distributions of boron, interstitials and vacancies following a 40 keV,  $2 \times 10^{14} \text{ cm}^{-2}$  B implant.

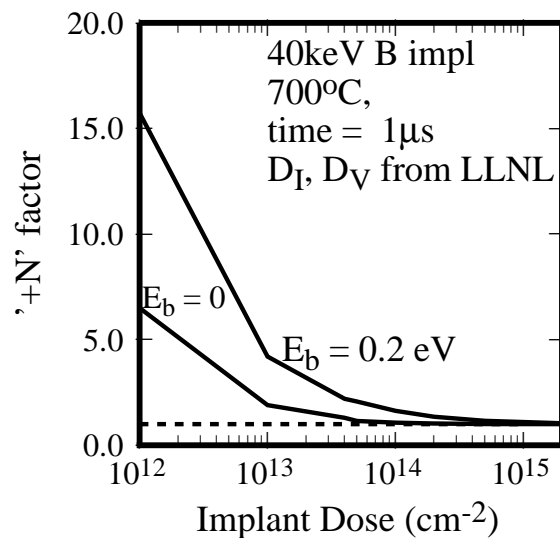


**Fig. 2:** Net interstitial dose remaining after the recombination process starting from the total initial defect distributions.  $E_b$  is the barrier to I/V recombination.

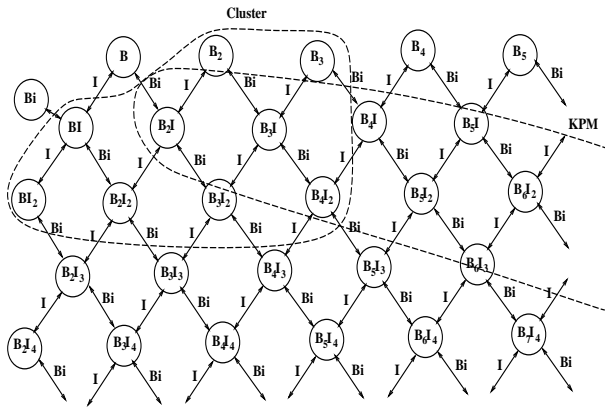


**Fig. 3:** Array of possible BICs. Also indicated schematically are the range of compositions considered by cluster and KPM approaches.

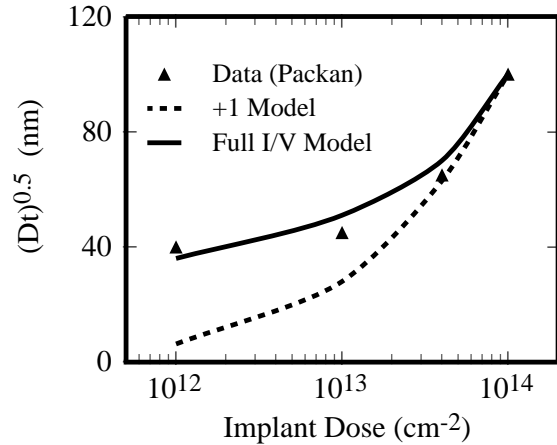


**Fig. 4:** Dose dependence of TED measured for a boron marker layer following 200 keV Si implants.

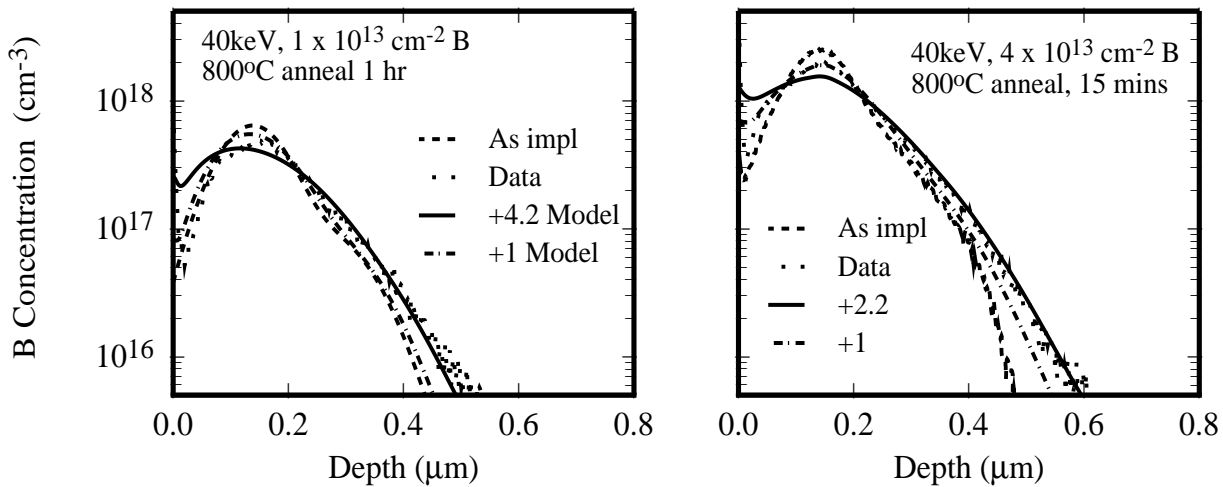


**Fig. 5:** Prediction of B TED for  $10^{13}$  and  $4 \times 10^{13}$   $\text{cm}^{-2}$  B implants. A '+1' model predicts less diffusion than seen experimentally.<sup>17</sup> A '+n' model based on the full initial defect profile is able to predict diffusion behaviour.

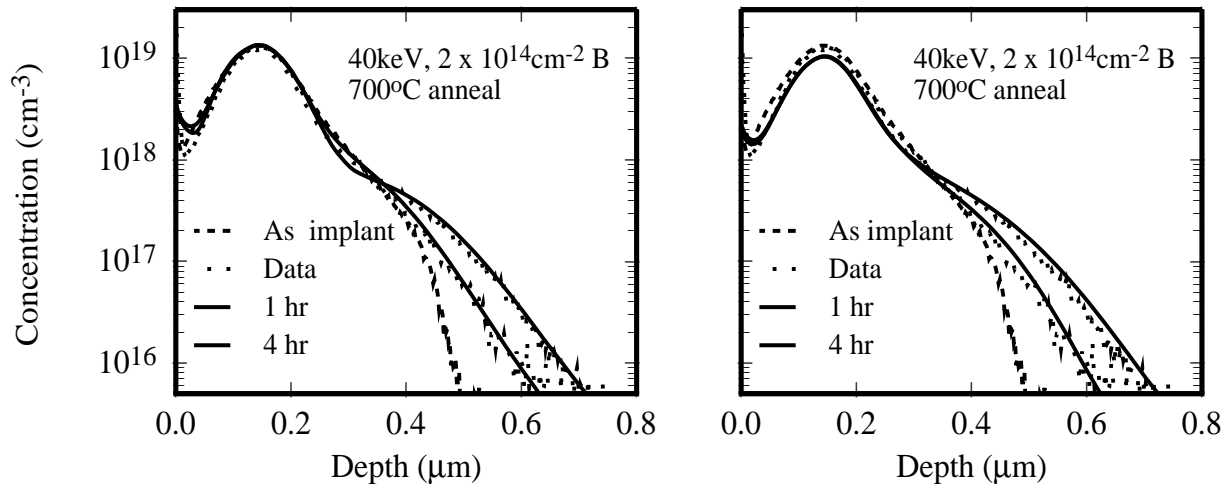


**Fig. 6:** Simulations results for a  $2 \times 10^{14}$   $\text{cm}^{-2}$ , 40 keV B implant annealed at 700°C with (a) KPM model and (b) Cluster model compared to data from Intel.<sup>17</sup>

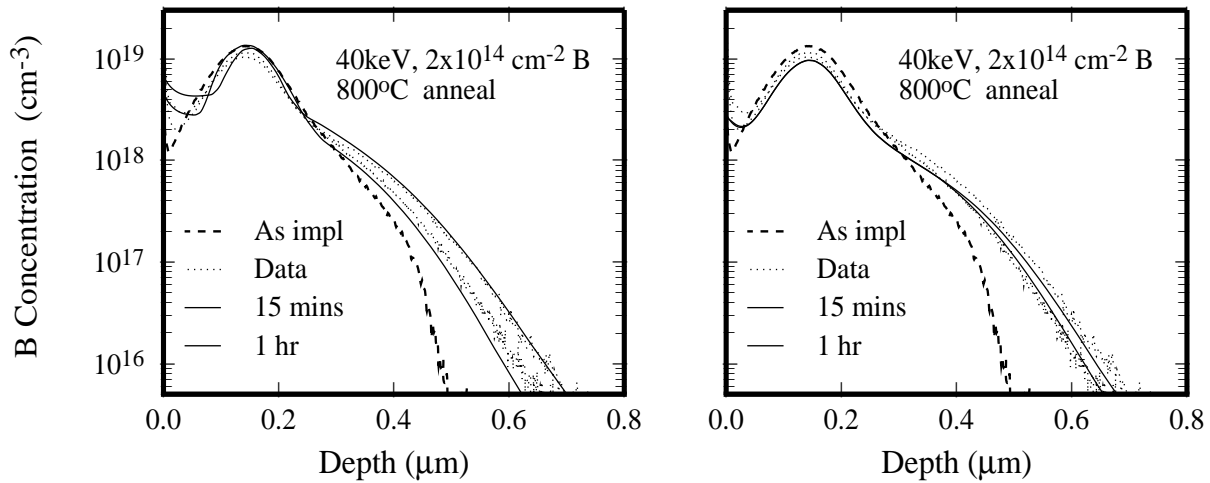


**Fig. 7:** Simulations results for a  $2 \times 10^{14} \text{cm}^{-2}$ , 40 keV B implant annealed at  $800^\circ\text{C}$  with (a) KPM model and (b) Cluster model compared to data from Intel.<sup>17</sup>

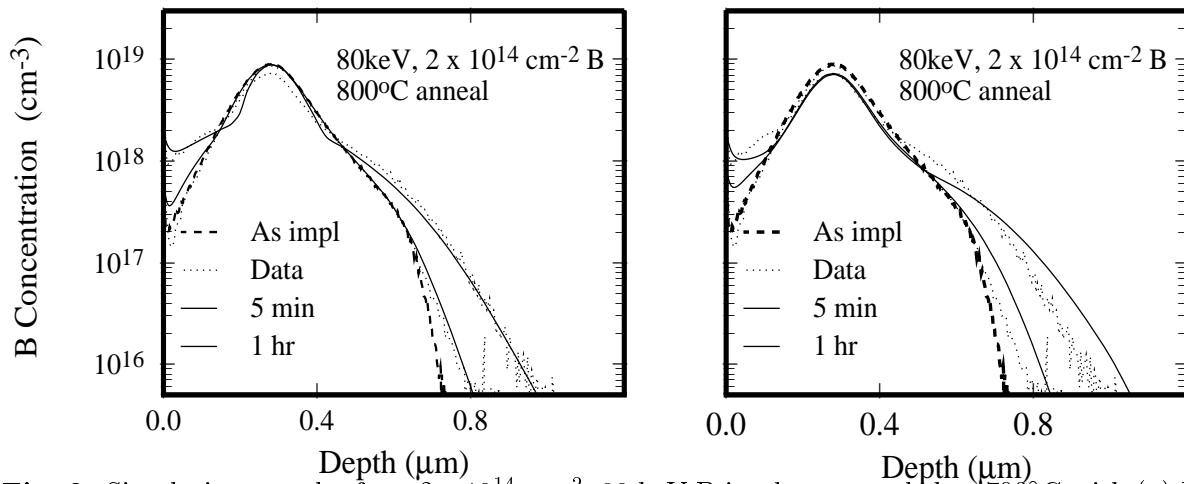


**Fig. 8:** Simulations results for a  $2 \times 10^{14} \text{cm}^{-2}$ , 80 keV B implant annealed at  $700^\circ\text{C}$  with (a) KPM model and (b) Cluster model compared to data from Intel.<sup>17</sup>

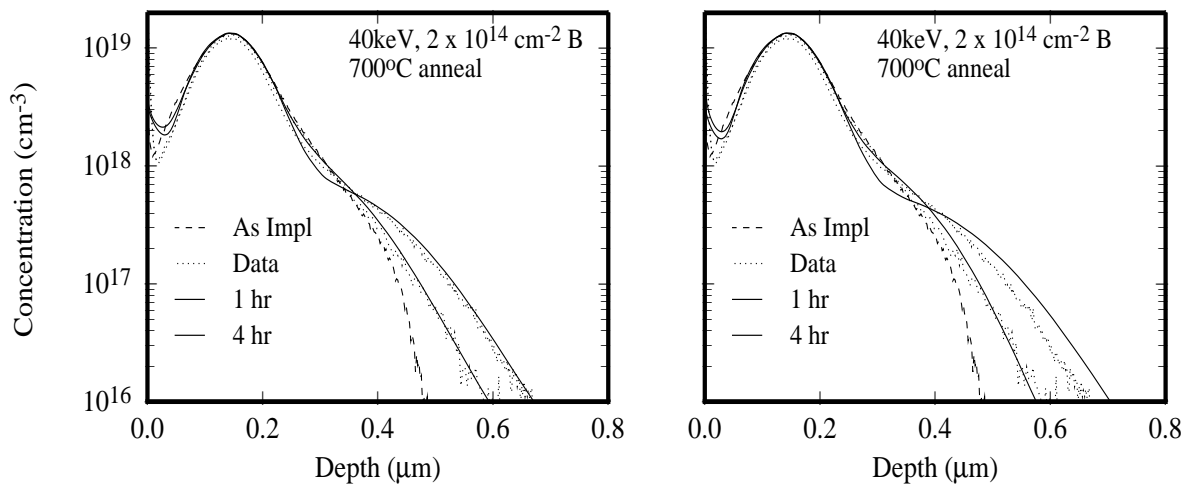


**Fig. 9:** Effect of  $\{311\}$  models on the evolution of the boron TED profiles for (a) a simple solubility model and (b) a moment-based model. Note that the moment-based model correctly captures the time dependence of TED as well as the evolution of the effective solid solubility (concentration from which tail diffusion takes off).